frontiers | Frontiers in Materials

ORIGINAL RESEARCH
published: 28 April 2022
doi: 10.3389/fmats.2022.855705

Modified Surface Composition and Biocompatibility of Core-Shell Nitinol Nanoparticles Fabricated *via* Laser Ablation of Differently Passivized Targets

Ujjwal Ranjan Dahiya[1], *Sonu Singh*[1], *Chetan Kumar Garg*[1], *Aakansha Rai*[2] *and Dinesh Kalyanasundaram*[1,3]*

[1]*Laboratory for Fabrication of Biomedical Devices, Centre for Biomedical Engineering, Indian Institute of Technology Delhi, New Delhi, India,* [2]*CSIR-Institute of Genomics and Integrative Biology (IGIB), New Delhi, India,* [3]*Department of Biomedical Engineering, All India Institute of Medical Sciences, New Delhi, India*

OPEN ACCESS

Edited by:
Yogendra Kumar Mishra, University of Southern Denmark, Denmark

Reviewed by:
Joana Claudio Pieretti, Federal University of ABC, Brazil
Eleonore Fröhlich, Medical University of Graz, Austria

***Correspondence:**
Dinesh Kalyanasundaram
dineshk.iitdelhi@gmail.com

Specialty section:
This article was submitted to Biomaterials, a section of the journal Frontiers in Materials

Received: *15 January 2022*
Accepted: *17 March 2022*
Published: *28 April 2022*

Citation:
Dahiya UR, Singh S, Garg CK, Rai A and Kalyanasundaram D (2022) Modified Surface Composition and Biocompatibility of Core-Shell Nitinol Nanoparticles Fabricated via Laser Ablation of Differently Passivized Targets. Front. Mater. 9:855705. doi: 10.3389/fmats.2022.855705

Nitinol is a versatile alloy known for its shape memory effect and thus finds multiple applications in biomedical devices and implants. The biomedical applications of nitinol-based devices are, however, limited because of concerns related to leaching and its associated cytotoxicity. In particular, nitinol nanoparticles (NPs), despite being highly promising for biomedical applications such as nano-actuators and biomolecular delivery agents are not explored, owing to the same concerns. Moreover, nitinol nanoparticles and their biological interactions are not fully characterized, and the available literature on their toxicity portrays a divided picture. Surface passivation of nitinol using multiple methods has been explored in the past to reduce the leaching of nickel in implants while also improving the thrombogenic properties. In this work, we reported the preparation of passivized nitinol NPs by laser ablation of nitinol targets, followed by different surface treatments. The effect of different treatments in reducing nickel leaching and its influence on biocompatibility were studied. The biocompatibility and multi-faceted interaction of nitinol NPs with osteoblast cells and associated toxicity were explored. Homogenous nitinol NPs were found to be generated at 25 W of laser power. Also, surface modification using hydrogen peroxide, anodization, and acid etching was found to be effective in waning the nickel leaching and improving biocompatibility. In view of the observed results of cellular interactions, we discussed the possible routes of cellular toxicity of these NPs. The prospective applications of such passivized NPs in the biomedical field are also discussed in this work.

Keywords: nickel-titanium, passivized nanoparticles, core-shell nanoparticles, cytotoxicity, MG63 osteoblast, cellular pathways, apoptosis

INTRODUCTION

Nitinol is a shape memory alloy made from nickel and titanium and has the ability to restore its original shape after deformation (Bhardwaj et al., 2019). Shape memory effects have been observed during austenite to martensite transformation, i.e., transformation from the *face-centered cubic* (FCC) structure to a *body-centered tetragonal* (BCT) structure (Parmar et al., 2021). Nitinol has gained popularity in the biomedical field, given its corrosion resistance, acceptable biocompatibility, super-elasticity, osseointegration, and fatigue and kink resistance properties (Hamann et al., 2020; Ulacia et al., 2020). The alloy has applications in the biomedical field as coronary stents, dental archwires, and actuators, although the concerns of nickel leaching limit the application (Fouladian et al., 2021).

To address the issue of possible nickel leaching from implants and reduce thrombogenicity, researchers have explored various surface treatments (passivation) viz. acid etching *via* HNO3, heat treatment, hydrogen peroxide treatment, mechanical rubbing, etc. (Norouzi and Nouri, 2021). It is believed that such surface treatments on nitinol result in changes in the surface composition of the alloy, where the percentage of nickel is reduced while that of Ti and TiO_2 becomes enhanced (Pérez et al., 2009; Norouzi and Nouri, 2021). Many reports in the literature have characterized the surface compositions of passivized nitinol and reported the presence of a titanium oxide layer (TiO_2), which can be explained in view of the favorable free energy for the formation of TiO_2. The presence of the oxide layer prevents corrosion of bulk materials and serves as a physicochemical barrier for Ni oxidation by modifying the oxidation pathways (Pulletikurthi et al., 2015). The effect of heat and electropolishing on the corrosion resistance in Hank's physiological solutions was studied in different medical-grade titanium and nitinol. Ti6AI4V was found to be the most resistant to corrosion, while nitinol yielded the highest resistance to chemical breakdown (Chakraborty et al., 2019). *In vitro* and *in vivo* studies indicated that passivized nitinol exhibited good biocompatibility and does not promote toxic or genotoxic reactions when in contact with a physiological environment (Gill et al., 2015). Therefore, passivized nitinol can be considered a biologically safe implant material with unique mechanical properties. It is a well-characterized fact that material property and biological interaction drastically change between macro to the nanoscale, which emphasizes the detailed exploration of nanoparticles (NPs) of new materials (De Oliveira et al., 2017; Safranski et al., 2020). NPs for biomedical applications can be manufactured from both organic and inorganic materials. They have been explored for bio-sensing, purification of biomolecules, bioimaging, targeted delivery of biomolecules, anticancer agents, hypothermic agents, diagnostics, theranostics, and biosensing (McNamara and Tofail, 2017; Dembski et al., 2018; Pugazhendhi et al., 2018; Dahiya et al., 2021). All the applications of NPs have been made possible, thanks to the multi-dimensional properties, given its nanoscale size, high surface charge, tailorable surface properties, high agent loadings, controllable release patterns, and enhanced permeability and retention effect (Ealias and Saravanakumar, 2017; Loza et al., 2020; Zelepukin et al., 2021). Organic NPs such as liposomes, dendrimers, and micelles are less stable at high temperatures while inorganic NPs fabricated from metallic substrates (e.g., Al, Cd, Cu, Ti, Zn, Au, Ag) or metallic alloys (NiTi, FeNi, and FePt) or metallic oxides (Fe_2O_3 and Al_2O_3) are stable at high temperatures (Kashapov et al., 2021). Hence, inorganic NPs are more suitable for hypothermia-based cancer-killing and extendable to applications demanding a wide temperature range of operation. Inorganic NPs exhibit near-perpetual physical, chemical, and biological properties that have been exploited for industrial applications including additives, pigments, dyes, catalysts, biomaterials, and antimicrobial additives. (Jeevanandam et al., 2018; Cui et al., 2020). For the purpose of biomedical applications, it is important to prepare stable monodispersed solutions with NPs possessing less aggregation propensity (Phan and Haes, 2019). The exposure of NPs in a physiological environment leads to absorption of biological substances (proteins, lipids, peptides, nucleic acids, metabolites, and others) onto the surface of the NPs, leading to the formation of biocorona (Shannahan, 2017; Ulacia et al., 2020). The biocorona presents a unique challenge for the practical and safe biomedical application by affecting the toxicity, functionality, and characteristics of NPs and thereby altering thrombogenic properties as well (Chakraborty et al., 2019; Sena et al., 2020).

Even beyond the passivation aspect, researchers have raised some concerns about the safe handling of Ni-based NPs, compared to the bulk material. Crosera et al., 2016 also confirmed factors that affect the accumulation of Ni ions on the skin surface, especially in the case of NPs (Crosera et al., 2016). Ion et al. showed that surface nitriding through superficial treatment is an excellent method to enhance the biocompatibility of implantable devices (Ion et al., 2016). It was shown that passivized implants improved the interfacial bonding of human umbilical vein endothelial cells (HUVECs), cell spreading, and proliferation. Another group of researchers introduced a new one-step method, ultrasonic nanocrystal surface modification (UNSM), to fabricate hierarchical surface structures on the nitinol alloy to enhance the interaction between cells and implants and thus increase their biocompatibility (Hou et al., 2018; Osfouri and Rahmani, 2021). Anodization followed by chitosan coating of nitinol NPs was reported to result in improved biocompatibility and corrosion resistance (Mohammadi et al., 2019). Nitinol wire electropolishing before braiding enhanced *in vitro* behavior with lower activation of coagulation and a tendency toward reduced platelet adhesion (Cattaneo et al., 2019).

In this work, core-shell NPs of nitinol were prepared by nanosecond laser irradiation of differently passivized substrates. About 10 different surface treatments were employed in passivizing the nitinol targets for the fabrication of different NPs. The biocompatibility and cellular toxicity of these diversely prepared particles were assessed in detail by studying their effect on cellular pathways. The mechanism underlying the cellular toxicity of these nanoparticles was assessed through MTT and DCFDA assay (intracellular ROS) measurements while discussing the

TABLE 1 | Preparation of different passivized targets of nitinol through multiple treatment methods.

A	Pre-removal of the oxide layer using Kroll's reagent				
B	**Type of passivation**	**Sample ID**	**Passivation treatment**	**Method**	**References**
	Unpolished	UpUT	No treatment		[51]
	Mechanically polished	PpUT	Polishing of the samples	Polishing all surfaces of targets by 3,000 grade abrasive paper	
	Heat	UpHT	Heat treatment	Treatment of nitinol targets in a muffle furnace @ 600°C for 30 min	[35,36]
	Polished + heat	PpHT	Mechanical polishing followed by heat treatment		
	HNO_3	$UpHNO_3$	Acid etching using nitric acid treatment	Nitinol targets to be submerged in 20% nitric acid solution @80°C overnight	[37,38]
	Polished + $HN0_3$	$PpHNO_3$	Mechanical polishing followed by nitric acid treatment		
	H_2O_2	UpH_2O_2	Passivation using hydrogen peroxide	Nitinol targets submerged in 30% Hydrogen peroxide solution under boiling condition for 2 h	[39,40]
	Polished + H_2O_2	PpH_2O_2	Mechanical polishing followed by hydrogen peroxide		
	Anodized	UpAND	Anodization in ammonium fluoride (NH_4F) in ethylene glycol as an anodizing solution	Anodization is carried out for 15 min at 60 V under a continuous ultrasonication bath. The concentration of NH_4F is 0.5 g/ml in ethylene glycol solution supplemented with 2% DI water	[41,42]
	Polished + anodized	PpAND	Mechanical polishing followed by anodization		

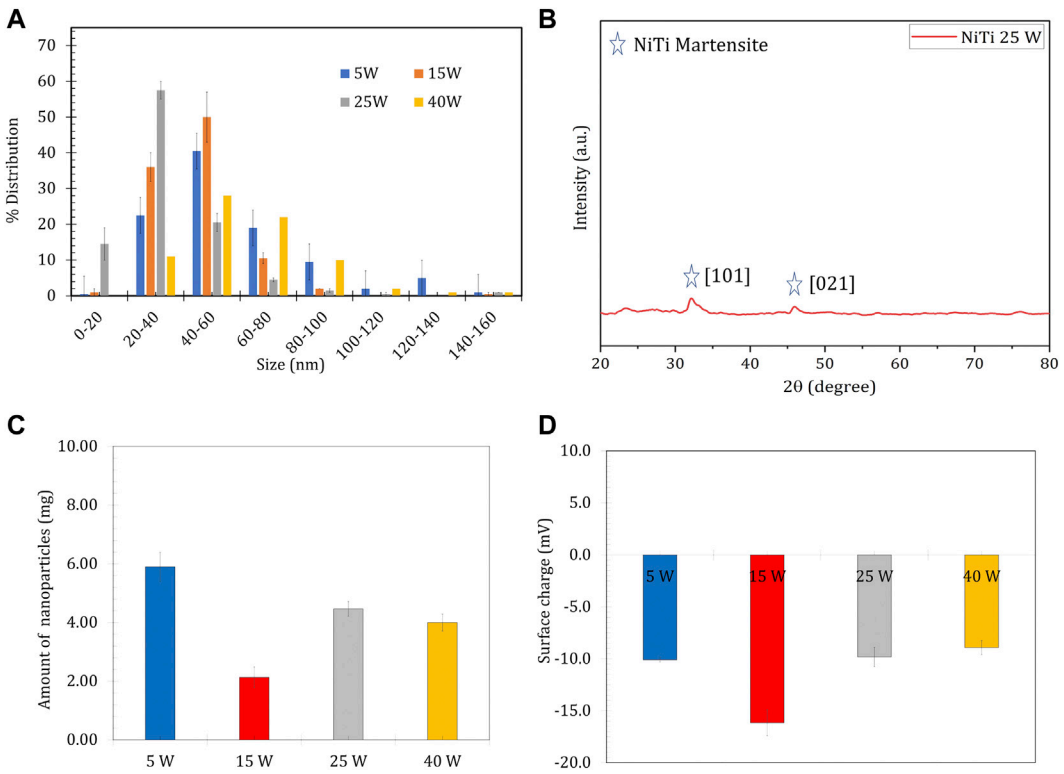

FIGURE 1 | Characterization of nitinol NPs prepared at different laser powers of 5, 15, 25, and 40 W **(A)** Distribution of the size of NPs estimated using ImageJ analysis **(B)** XRD spectra of nitinol nanoparticles prepared *via* 25 W laser power **(C)** Yield of NPs prepared at different laser powers and **(D)** Surface charge (zeta potential) measurement of different preparations.

contributing alternative biological pathways. NPs fabricated using targets that were passivized using either chemical treatment (using HNO_3 and H_2O_2), anodization, or thermal heating were found to result in reduced nickel leaching in the media and improved biocompatibility. Given the obtained results and available literature studies, effective treatments for producing biocompatible NPs of nitinol are discussed along with its prospective application in the biomedical field.

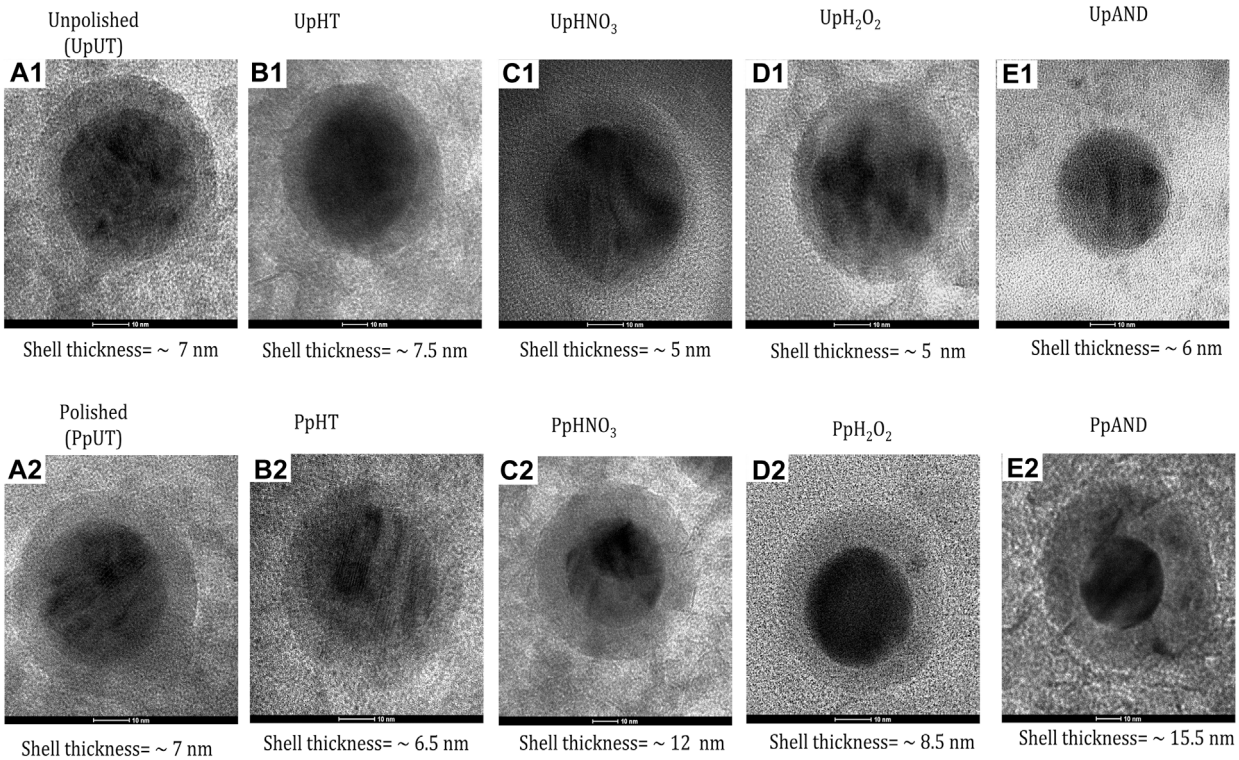

FIGURE 2 | HR-TEM Characterization of Passivized Nitinol. (A1-E2) High-Resolution Transmission Electron Microscopy (TEM) images of single passivized nitinol nanoparticle.

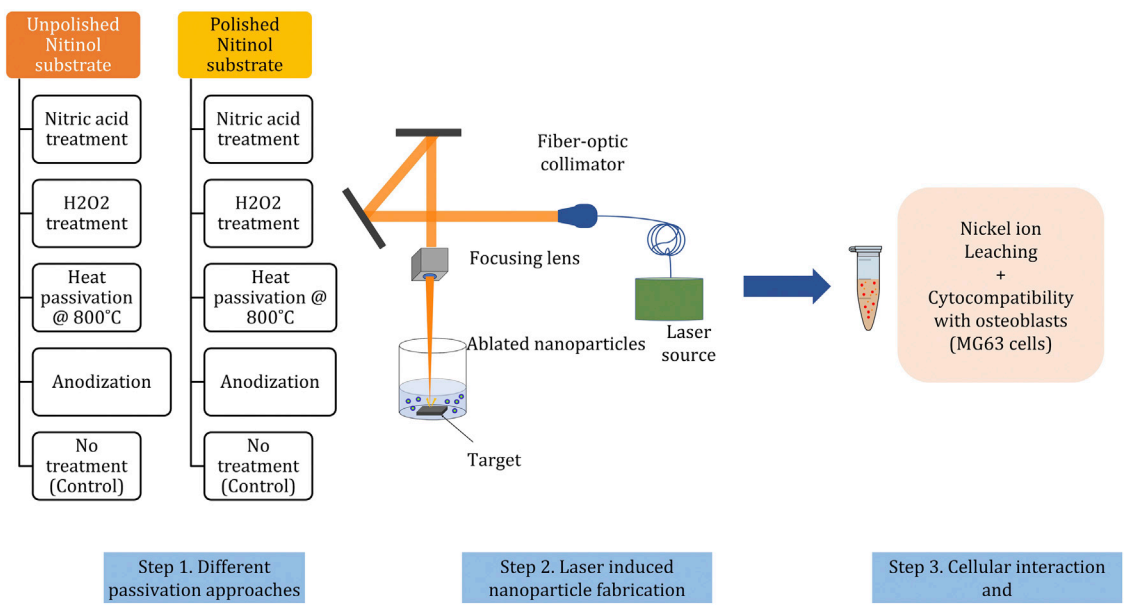

FIGURE 3 | Workflow for studying the effect of surface treatments (passivation) of nitinol targets on nickel leaching and cytocompatibility of corresponding ablated NPs. In brief nitinol targets are subjected to four different surface treatments with or without mechanical polishing, resulting in a total of ten differently treated nitinol surfaces.

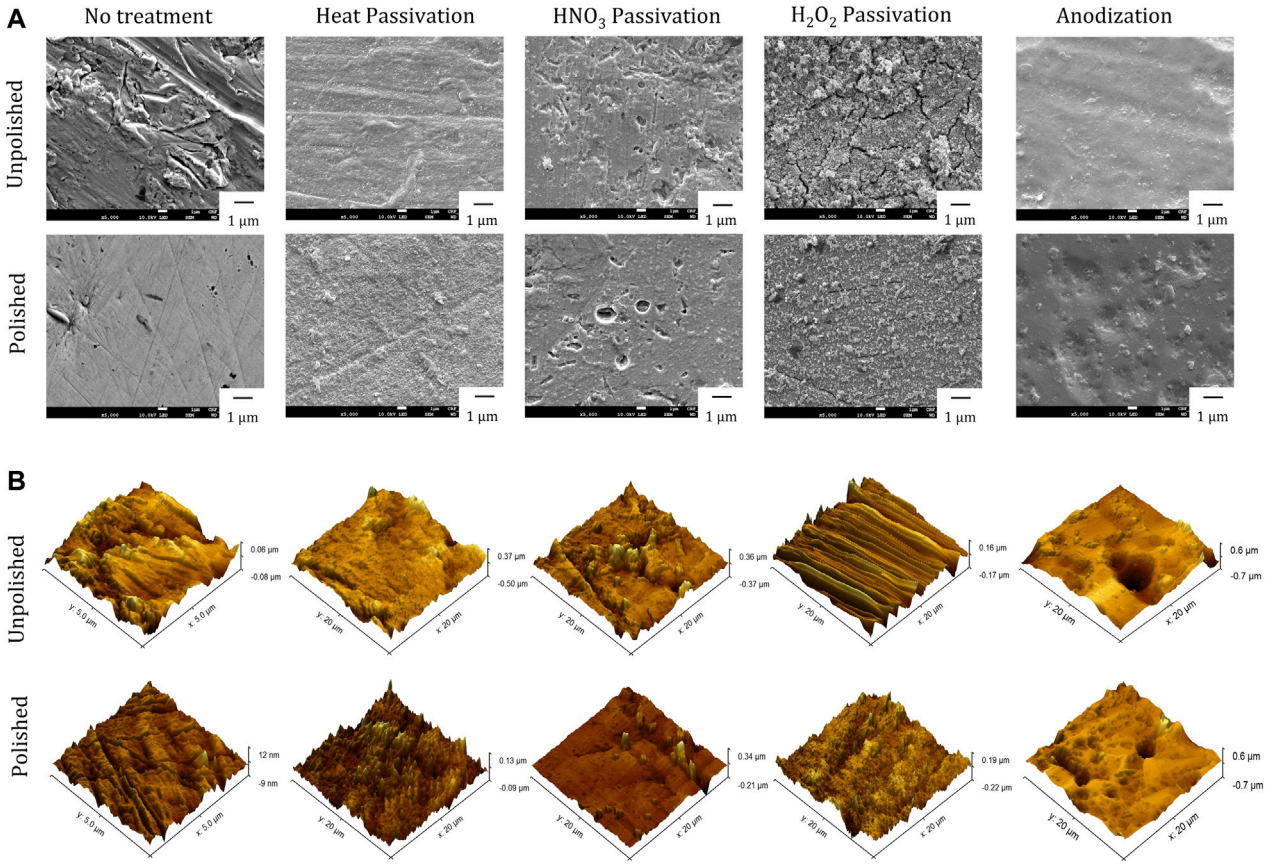

FIGURE 4 | Surface characterization of passivized nitinol targets **(A)** Scanning Electron Microscopy (SEM) imaging and **(B)** Atomic Force Microscopy (AFM) imaging for nitinol targets after different Passivation treatments.

MATERIALS AND METHODS

Preparation and Passivation of Nitinol Targets

Nitinol samples of 10 mm × 10 mm were cut from commercially available nitinol plates of thickness 2 mm using a 400-W fiber laser machine (laser source model: R4 Series; maker: SPI Lasers Limited, UK). These nitinol samples were polished using 400, 600, 1,000, and 1,200 grade abrasive papers. The prepared targets were treated with Kroll's reagent solution (40% hydrogen fluoride and 40% nitric acid) overnight to remove the preformed oxide layers (Kum and Chang, 2017; Sena et al., 2020). Ten sets of nitinol targets were prepared out of which five sets were mechanically polished using 3,000 grade abrasive paper (Group A) while the remaining were used without polishing (Group B). Four different passivation procedures were carried out on each group sample, namely, heating in a muffle furnace [600°C for 30 min (Oncel and Acma, 2017; Nagaraja and Pelton, 2020)], HNO_3 treatment [20% HNO_3 acid for 12 h at room temperature (Mirjalili et al., 2013; Norouzi and Nouri, 2021)], H_2O_2 treatment (30% H_2O_2 for 2 h under boiling conditions (Chu et al., 2006; Shabalovskaya et al., 2012; Nagaraja and Pelton, 2020)), and anodization [60 V DC, 15 min in the presence of 0.5% of NH_4F eluted in a mixture of ethylene glycol with 2% DI water (Davoodian et al., 2020; Rahimipour et al., 2020)]. **Table 1** describes the details of the treatment. The change in the surface characteristics and the working of the passivation method were established through scanning electron microscopy (SEM, JEOL JSM-7800F Prime) and atomic force microscopy (AFM, Asylum Research MFP3D-BIO) used for capturing the topographical features.

Preparation of NPs From Passivized and Non-Passivized Targets

A nanosecond (*ns*) pulsed fiber laser (Model: SP-050-A-RM-Z-B-Y; Maker: SPI Lasers Limited, UK) of wavelength 1,060 ± 10 nm was used for the fabrication of nitinol NPs. The focused *ns* laser beam ablates the surface of the nitinol target placed in a 5-ml beaker filled with 1.2 ml of DI water. The level of the water is a couple of mm above the surface of the sample. The ablation experiments were carried out for 30 min. During the experiments,

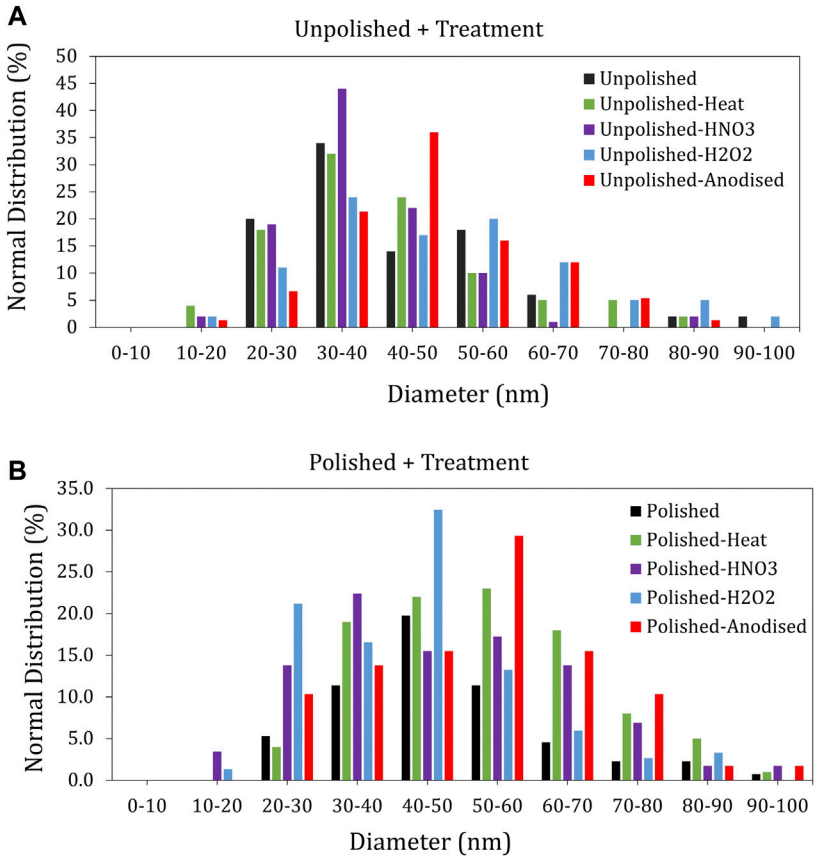

FIGURE 5 | Size distribution of nitinol NPs ablated from differently passivized nitinol targets characterized using ImageJ analysis of transmission electron micrographs **(A)** Distribution of size for unpolished samples. **(B)** Distribution of size for polished samples.

the DI water was replenished to approximately the same level (i.e., a couple of mm above the surface of the sample) to compensate for the evaporation of the liquid. Initially, the NPs were prepared by ablating the un-passivized targets at an average laser power of 5, 15, 25, and 40 W. Based on these initial experiments, 25 W was found to be the most optimal. Hence, for all the subsequent experiments, 25 W was used for the preparation of the ten sets of NPs. The detailed laser parameters used to fabricate the NPs are given in **Supplementary Table S1** of the supplementary section.

Characterization of NPs

The amount of NPs generated at different laser powers was estimated by drying the samples on a heating block, followed by resuspension in 100 µL of water. A calibrated scale and 200-µL microfuge tubes were used to estimate the yield of the ablated NPs. To assess any possible effect of the surface treatment of nitinol targets on the size distribution of ablated NPs, transmission electron microscopy (TEM) was performed for all ten types of NP preparations. A suspended nanoparticle solution was drop-cast on carbon-coated copper grids, and the samples were analyzed using TEM (JEOL JEM-1400) and images were captured on a 200-nm scale. At least five frames were captured at 1,000X magnification to ensure 100 particles for estimating the size distribution. ImageJ® software was used for analyzing the captured images and obtaining the size distribution. To analyze the relation between cellular toxicity and nanoparticle morphology, high-resolution transmission electron microscopy (HRTEM, FEI Tecnai TF20) of single nanoparticles was carried out.

Effect of Passivation on Cytotoxicity of Nitinol NPs

Cellular viability was estimated using an MTT assay in the murine osteoblast cell line MG63. After treating the cells with different volumes of nitinol NPs, the MG63 cells were seeded at a density of 40,000 cells per well in a 500 µL DMEM culture medium with 10% FBS in 24-well plates followed by incubation at 37°C. After 24 h, the cells were treated with different concentrations of nitinol nanoparticles in serum-free media (Opti-MEM) for 4 hours. After 4 h of incubation, the NPs were removed, and the cells were washed with 1X PBS, followed by the addition of 1 ml of fresh DMEM media to each well. After 24 h, 300 µL of an MTT reagent (of concentration 1 mg/ml) was added to the media and further incubated for 3 h. The purple formazan crystals thus formed were dissolved in 100 µL dimethyl sulfoxide (DMSO).

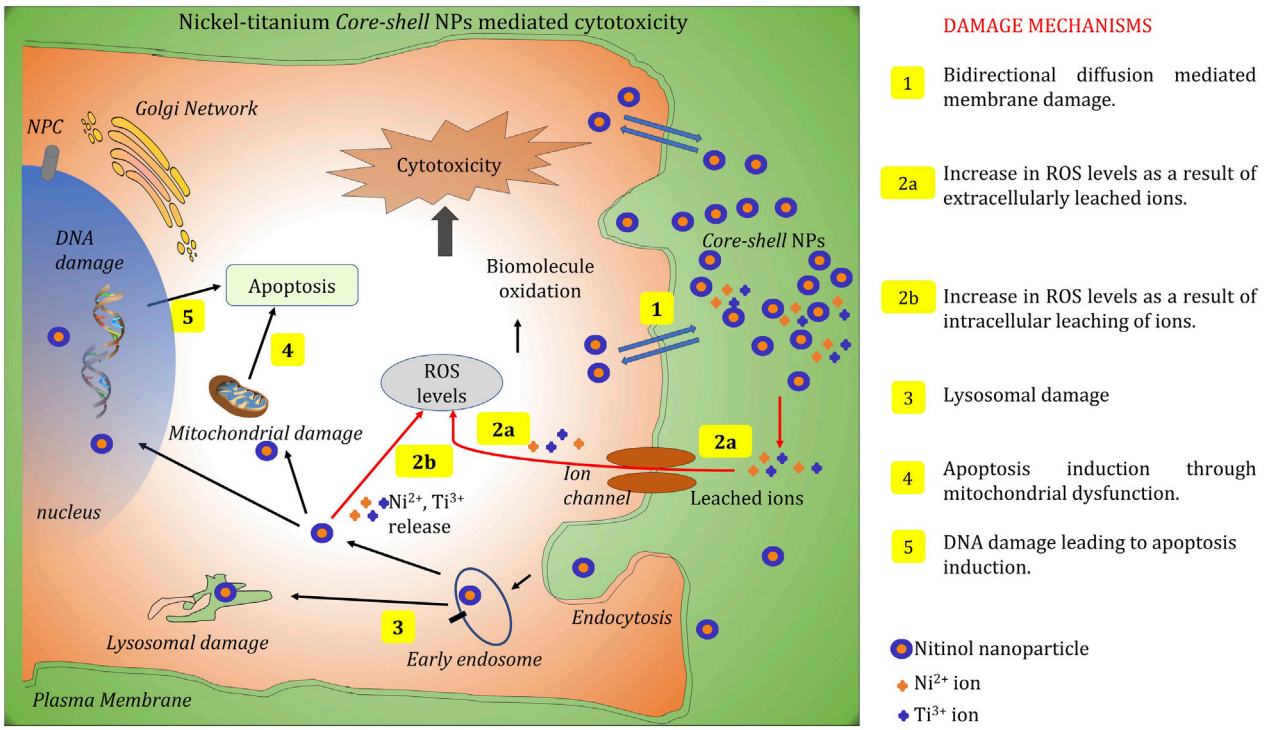

FIGURE 6 | Summary of different molecular pathways through which NPs can cause cellular toxicity. Five distinct molecular mechanisms have been illustrated in the schematic representation which represents the major pathways through cellular interaction of NPs that can lead to cell death.

The absorbance was measured using an ELISA reader at a wavelength of 540 nm and a reference wavelength of 620 nm. The percentage of viable cells was expressed considering untreated cells as 100% viable. The cells were found to tolerate 100 ng/μL of nitinol NPs without significant cytotoxicity (**Supplementary Figure S1**). To study the effect of passivized NPs, 100 ng/μL of differently passivized nanoparticles was used, and an MTT assay was performed as discussed previously.

Ni Ion Leaching Using ICP-MS

Characterization of nickel leaching from the passivized NPs was performed using the ICP-MS approach. For ICP-MS measurements, the freshly prepared passivized nitinol NPs were harvested by centrifugation at 10,000 g suspended in 1 ml of DMEM media supplied with 10% FBS and kept in a BOD incubator at 37 °C for 24 h. Post-incubation, the solution was centrifuged, the NPs were removed, and the solution was diluted to 5 ml using nuclease-free water. This solution was then used for ICP-MS measurement.

Intracellular ROS Measurement Through CM-H_2 Dichloro Fluorescein Di-Acetate Assay

The MG63 osteoblast cells were seeded in a 24-well plate at a density of 50,000 cells/well and allowed to grow for 24 h in a 5% CO_2-enriched humidified incubator at 37°C to attain a subconfluent condition (~70%). The cells were then treated with 10 μg/ml of NPs in Opti-MEM (serum-free media) for another 4 h, subsequent to which the cells were allowed to grow for another 20 h after changing the media. The cells were then treated with 10 μM of H_2DCFDA for 20 min, followed by two consecutive washes with cold 1X PBS, trypsinization, and a final suspension in 200 μL of PBS. Cellular processing was performed at 4°C (on ice) to prevent osmotic lysis. The cellular suspensions were finally analyzed for ROS production using the BD Accuri Flow cytometer (BD. Biosciences, United States).

Statistical Analysis

All the experimental evaluations are shown by means of the readings and the standard deviation. A non-parametric *t-test* was used for estimating the difference between treatments using GraphPad Prism 6® software. A p value of less than 0.05 was considered to be significant. In all of the graphical representations, the following symbols were used: $^{*}p < 0.05$, $^{**}p < 0.01$, $^{***}p < 0.001$, and *ns*, not significant.

RESULTS AND DISCUSSIONS

Nitinol targets were ablated using a nanosecond laser at four different fluences (Table S1) in 1.2 ml of DI water. The size distribution profile suggested a more homogenous nanoparticle preparation at the average powers of 15 and 25 W in comparison

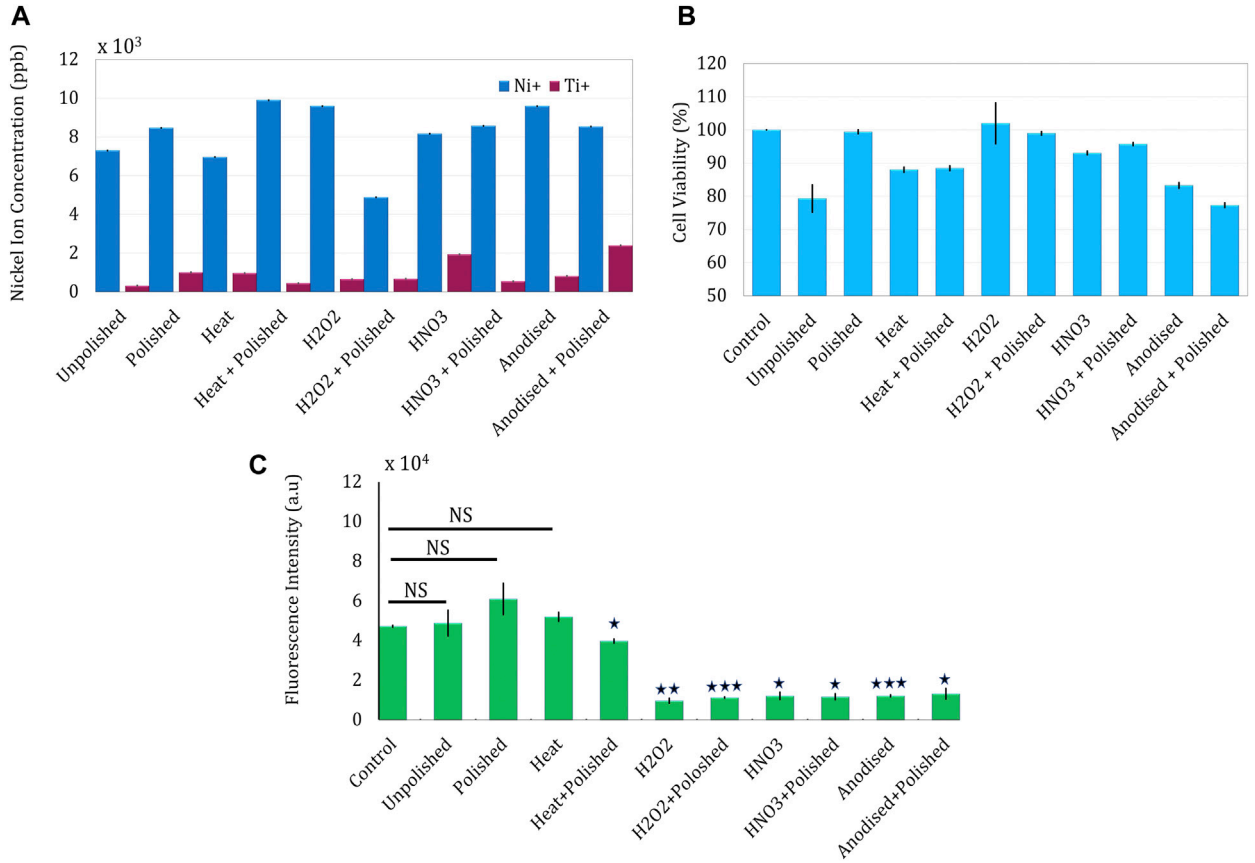

FIGURE 7 | Estimation of nickel leaching and corresponding cellular interaction of nitinol NPs prepared after laser ablating different passivized targets. **(A)** Core-shell nitinol particles and leaching of nickel ions from the particles estimated using the ICPMS method **(B)** Estimation of cellular toxicity of passivized NPs on MG63 osteoblast cells **(C)** Intracellular ROS estimation in MG63 cells after treating with NPs for 4 h.

with 5 and 40 W laser power, respectively (**Figure 1A**). Higher yields of ablated NPs were observed at 5 and 25 W laser power (**Figure 1C**). The prepared nitinol NPs showed a negative surface charge regime (**Figure 1D**) and characteristic phase peaks on an XRD analysis (**Figure 1B**). The resultant NPs were found to have a core-shell arrangement, as seen through HR-TEM imaging (**Figure 2**). The obtained characterizations on nitinol NP preparation suggested the use of 25-W laser power as the optimal operating power. The fabricated nanoparticles showed negligible aggregation propensity, as suggested by dynamic light scattering (DLS) measurement for 24 h (**Supplementary Figure S2**).

The effect of different passivation procedures (surface treatments) on enhancing the biocompatibility of nitinol NPs ablated from the substrates was studied. The study design for generating passivized NPs and to compare their effect on biocompatibility is summarized in **Figure 3**. Before either mechanical or chemical treatment, all the substrates were subjected to Kroll's reagent, as described in the materials and methods section. This ensured the removal of the oxide layer on the substrates to minimize any variation between these. A total of 10 diverse NPs were studied from different surface treatments. FESEM-based imaging of the substrates post treatments showed different and distinct surface features (**Figure 4A**). Deep craters were observed post HNO_3 treatment with or without pre-polishing. Similarly, distinctly different surface cracks were found post H_2O_2 treatment with or without pre-polishing. A 3D topography map for all surfaces was observed by atomic force microscopy (AFM). The highest *Z*-axis (vertical) variation was observed post anodization of the samples (with or without pre-polishing) (**Figure 4B**). This observation was in line with the available literature on anodization, which suggests the growth of tubular TiO_2 structures on titanium and nitinol substrates during anodization [38]. Pre-polishing was found to reduce vertical anomalies, and the nitinol target subjected to pre-polishing yielded minimal *z*-axis variation.

Different nitinol substrates were subjected to ns laser ablation (25 W power), as described earlier for generating passivized NPs. The size distribution of these differently passivized NPs was then characterized with TEM imaging followed by ImageJ analysis, and the NPs ablated from HNO_3-etched surfaces (without pre-polishing) were found to have a comparatively narrow size distribution (20–60 nm) (**Figure 5A**). Narrow size distribution (20–60 nm) was also seen for particles ablated from PpH_2O_2

TABLE 2 | Surface passivation parameters and the overview of the resultant biological interactions on MG63 osteoblasts.

	Untreated	Mechanically polished	Heat	Polished + heat	HNO_3	Polished + HNO_3	H_2O_2	Polished + H_2O_2	Anodization	Polished + anodization
1. Nickel leaching (ppb)	7,300	8,466	6,960	9,904	8,168	8,571	9,596	4,880	9,594	8,534
2. Intracellular ROS generation by DCFDA assay (fluorescence intensity)	49K	60K	52K	40K	12K	12K	10K	11K	12K	13K
3. MTT assay (%)	80	100	88	88	102	99	93	96	83	77
Overall toxicity	High	Low	Slightly high	Slightly high	Low	Low	Low	Low	Slightly high	High
Comments	ROS levels are higher; however, MTT assay toxicity differs in polished samples. This indicates that cells may soon become unviable.		ROS levels are high, Ni + ion leaching is high, and MTT assay viability is less than 90%. Hence, we can conclude that cellular toxicity is HIGH.		ROS levels are low, Ni + ion leaching is low, and MTT assay viability is close to 100%. Hence, we can conclude that cellular toxicity is LOW.		The substantial effect of Ni + ion leaching is not observed.		Even though Ni + ion leaching is low and ROS levels are also low, the cellular toxicity is high. Other pathways such as mitochondrial damage and genotoxicity might have affected the cell viability.	

[a]*NA, not assessed.*

[b]*High, low, and normal—with respect to values observed for untreated nanoparticles.*

surfaces (**Figure 5B**). Interestingly, the particles ablated from $PpHNO_3$ surfaces showed wide size distribution.

NPs when used in biological applications can interrupt the typical structure and function of the tissue and organ and disrupt the normal physiology of the tissue. The particle size, shape, and composition are significant factors affecting toxicity (Canta and Cauda, 2020). Because of their small size, NPs permeate the cell membrane and spread to both the cardiovascular and lymphatic systems. The NPs accumulate in various tissues and interact with the cellular structure. The NPs also interact with proteins and may cause devastating consequences by creating protein corona on their surfaces, which causes deprivation of essential proteins and metabolites required for cell maintenance (Hoshyar et al., 2016; Curenton et al., 2021). Thus, it is important to understand the biocompatibility of NPs for a given application, by gaining insights into hemocompatibility, histocompatibility, and toxicity (Interactions et al., 2019). The size and polydispersity of nanoparticles also play an important factor in determining the cellular uptake and intracellular localization of nanoparticles, thereby associated toxicity pathways (Dahiya et al., 2019). Before extending any nanoparticles for putative biomedical application and related roles, it is imperative to understand the associated toxicity and the probable mechanistic alterations in the target tissues (Kyriakides et al., 2021).

The available literature on the biocompatibility and toxicity of nitinol portrays a well-divided opinion because of which its applicability and progress in the field are hampered (Sevost'yanov et al., 2018; Hamann et al., 2020). Hahn et al. reported higher cytotoxicity of nitinol NPs in comparison with other metal alloy NPs (Hahn et al., 2012; Puttaramaiah et al., 2021). To understand the bio-interaction and possible cytotoxicity, pathways related to nanoparticle-associated toxicity that can lead to cellular death and damage are identified and shown in **Figure 6**. To understand the mode of cellular toxicity of nitinol NPs and how surface passivation of these NPs impacts their cytocompatibility, cellular studies were performed with MG-63 osteoblast cells. The most challenging aspect of using nitinol in biological applications and as stents is the concern of nickel release. Characterization of nickel leaching from these passivized NPs was performed using the ICP-MS approach. The nitinol target was ablated for 30 min while being submerged in a thin layer (approximately 1 cm) of water above it, resulting in the formation of NPs in the solution. For an ICP-MS-based estimation of ion leaching, the prepared particles were harvested by centrifugation and resuspended in 1 ml of DMEM media (enriched with 10% FBS) followed by incubation for 24 h at 37°. The amount of leached ions was then measured in the supernatant.

Overall, nickel leaching was found to be more prominent and varying than titanium leaching across all sample types (**Figure 7**). A decade of extensive research on metallic NP-based cytotoxicity has suggested the involvement of multiple pathways including the classical extrinsic or intrinsic apoptotic pathway, an intrinsic mitochondrial pathway for ROS generation, or the simple mechanical disruption of the cell wall (Chakraborty et al., 2019).

As suggested by the ICP-MS data, polishing + hydrogen peroxide treatment resulted in the lowest nickel leaching among the tested samples. Mechanical polishing of the target was found to produce NPs with a slightly higher toxicity

(7,300–8,344 ppb). As mechanical polishing was always the first treatment, it can be inferred from the ICP-MS data that heat and nitric acid treatments elevate nickel leaching, while hydrogen peroxide and anodization lead to lowering of nickel leaching. Even though the estimated values were not able to completely justify the corresponding cellular toxicity (largely owing to the involvement of other pathways), a significant correlation between the two can be observed (**Table 2**).

NPs ablated from the surface which is treated with HNO_3, H_2O_2, and anodization (with or without pre-polishing) were found to show very low intracellular ROS generation in the DCFDA assay. Yet another explanation of the observed discordance can be the presence of nanotubular structures (generated on anodization) on ablation, which can cause enhanced mechanical damage to the cell membrane and thus leading to toxicity. Both higher nickel leaching and intracellular ROS of heat-treated samples (with and without pre-polishing) justify the significant toxicity observed in these treatments.

We found that the cellular interaction of passivized and bare nanoparticles can be explained to a good extent with the help of ion leaching and intracellular toxicity. The possibility that these alloy NPs can also affect cellular proliferation through abstruse biological pathways persists (some of which have been discussed in **Figure 6**) and stresses the need for further studies. In essence, the present work showcases that the composition, ion leaching, and biocompatibility of nitinol NPs can be modulated by selective surface treatment prior to mechanical ablation.

CONCLUSION

Nitinol nanoparticles can be used in the biomedical field as pertaining to nano-actuators and in cell-specific applications; however, these particles are poorly explored in the domain of biological applications because of the associated concerns of cellular toxicity. On the contrary, bulk nitinol is widely used in medical implants and stents after surface modification (passivation). This work presents an attempt to prepare surface-modified nanoparticles of nitinol, by following a distinct approach of ablating the particles from passivized surfaces of nitinol. Cellular interaction studies on MG63 osteoblasts suggest intracellular ROS and nickel leaching as the major pathways of induced toxicity. The overall nanoparticles ablated from H_2O_2-treated nitinol targets were found to exhibit the highest biocompatibility with the cells, thus suggesting these treatments as effective in reducing nitinol nanoparticle toxicity. This study is a significant step toward preparing biocompatible nitinol for biomedical applications.

DATA AVAILABILITY STATEMENT

The original contributions presented in the study are included in the article/**Supplementary Material**; further inquiries can be directed to the corresponding author.

AUTHOR CONTRIBUTIONS

UD: research planning, experimental work, data analysis, and manuscript writing. SS: experimental work and manuscript writing. CG: experimental work. AR: biological assays. DK: supervision, manuscript writing, data evaluation, and analysis.

FUNDING

The reported research was supported by the Indian Council of Medical Research (5/3/8/47/2020-ITR) and the Indo-German Science and Technology Centre (IGSTC/Call 2014/Sound4All/24/2015-16).

ACKNOWLEDGMENTS

The authors acknowledge the Central Research Facility (CRF), IIT Delhi, and Nanoscale Research Facility (NRF), IIT Delhi, for various characterizations performed during this study.

SUPPLEMENTARY MATERIAL

The Supplementary Material for this article can be found online at: https://www.frontiersin.org/articles/10.3389/fmats.2022.855705/full#supplementary-material

REFERENCES

Bhardwaj, A., Gupta, A. K., Padisala, S. K., and Poluri, K. (2019). Characterization of Mechanical and Microstructural Properties of Constrained Groove Pressed Nitinol Shape Memory alloy for Biomedical Applications. *Mater. Sci. Eng. C* 102, 730–742. doi:10.1016/j.msec.2019.04.070

Canta, M., and Cauda, V. (2020). The Investigation of the Parameters Affecting the ZnO Nanoparticle Cytotoxicity Behaviour: A Tutorial Review. *Biomater. Sci.* 8, 6157–6174. doi:10.1039/d0bm01086c

Cattaneo, G., Bräuner, C., Siekmeyer, G., Ding, A., Bauer, S., Wohlschlögel, M., et al. (2019). *In Vitro* investigation of Chemical Properties and Biocompatibility of Neurovascular Braided Implants. *J. Mater. Sci. Mater. Med.* 30 (6), 67. doi:10.1007/s10856-019-6270-6

Chakraborty, R., Datta, S., Raza, M. S., and Saha, P. (2019). A Comparative Study of Surface Characterization and Corrosion Performance Properties of Laser Surface Modified Biomedical Grade Nitinol. *Appl. Surf. Sci.* 469, 753–763. doi:10.1016/j.apsusc.2018.11.045

Chethankumara, G. P., Nagaraj, K., Krishna, V., and Krishnaswamy, G. (2021). Isolation, Characterization and *In Vitro* Cytotoxicity Studies of Bioactive Compounds from Alseodaphne Semecarpifolia Nees. *Heliyon* 7 (6), e07325. doi:10.1016/j.heliyon.2021.e07325

Chu, C. L., Chung, C. Y., and Chu, P. K. (2006). Surface Oxidation of NiTi Shape Memory alloy in a Boiling Aqueous Solution Containing Hydrogen Peroxide. *Mater. Sci. Eng. A* 417, 104–109. doi:10.1016/j.msea.2005.11.010

Crosera, M., Adami, G., Mauro, M., Bovenzi, M., Baracchini, E., and Larese Filon, F. (2016). *In Vitro* dermal Penetration of Nickel Nanoparticles. *Chemosphere* 145, 301–306. doi:10.1016/j.chemosphere.2015.11.076

Cui, Z., Li, S., Zhou, J., Ma, Z., Zhang, W., Li, Y., et al. (2020). Surface Analysis and Electrochemical Characterization on Micro-patterns of Biomedical Nitinol after Nanosecond Laser Irradiating. *Surf. Coat. Tech.* 391, 125730. doi:10.1016/j.surfcoat.2020.125730

Curenton, T. L., Davis, B. L., Darnley, J. E., Weiner, S. D., and Owusu-Danquah, J. S. (2021). Assessing the Biomechanical Properties of Nitinol staples in normal, Osteopenic and Osteoporotic Bone Models: A Finite Element Analysis. *Injury* 52 (10), 2820–2826. doi:10.1016/j.injury.2021.08.006

Dahiya, U. R., Mishra, S., Chattopadhyay, S., Kumari, A., Gangal, A., and Ganguli, M. (2019). Role of Cellular Retention and Intracellular State in Controlling Gene Delivery Efficiency of Multiple Nonviral Carriers. *ACS Omega* 4 (24), 20547–20557. doi:10.1021/acsomega.9b02401

Dahiya, U. R., Gupt, G. D., Dhaka, R. S., and Kalyanasundaram, D. (2021). Functionalized Co2FeAl Nanoparticles for Detection of SARS CoV-2 Based on Reverse Transcriptase Loop-Mediated Isothermal Amplification. *ACS Appl. Nano Mater.* 4 (6), 5871–5882. doi:10.1021/acsanm.1c00782

Davoodian, F., Salahinejad, E., Sharifi, E., Barabadi, Z., and Tayebi, L. (2020). PLGA-coated Drug-Loaded Nanotubes Anodically Grown on Nitinol. *Mater. Sci. Eng. C* 116, 111174. doi:10.1016/j.msec.2020.111174

De Oliveira, D. P., Ottria, L., Gargari, M., Candotto, V., Silvestre, F. J., and Lauritano, D. (2017). Surface Modification of Titanium Alloys for Biomedical Application: From Macro to Nano Scale. *J. Biol. Regul. Homeost. Agents* 31 (2 Suppl. 1), 221–232.

Dembski, S., Schneider, C., Christ, B., and Retter, M. (2018). "5-Core-shell Nanoparticles and Their Use for *In Vitro* and *In Vivo* Diagnostics," in *Core-Shell Nanostructures for Drug Delivery and Theranostics*. Editors M. L. Focarete and A. Tampieri (Amsterdam, Netherlands: Elsevier), 119–141. doi:10.1016/b978-0-08-102198-9.00005-3

de la Harpe, K. M., Kondiah, P. P. D., Choonara, Y. E., Marimuthu, T., du Toit, L. C., Pillay, V., et al. (2019). The Hemocompatibility of Nanoparticles: A Review of Cell-Nanoparticle Interactions and Hemostasis. *Cells* 8 (6), 1–25. doi:10.3390/cells8101209

Ealia, S. A. M., and Saravanakumar, M. P. (2017). A Review on the Classification, Characterisation, Synthesis of Nanoparticles and Their Application. *IOP Conf. Ser. Mater. Sci. Eng.* 263 (3), 032019. doi:10.1088/1757-899X/263/3/032019

Fouladian, P., Jin, Q., Arafat, M., Song, Y., Guo, X., Blencowe, A., et al. (2021). Drug-loaded, Polyurethane Coated Nitinol Stents for the Controlled Release of Docetaxel for the Treatment of Oesophageal Cancer. *Pharmaceuticals* 14 (4), 311. doi:10.3390/ph14040311

Gill, P., Musaramthota, V., Munroe, N., Datye, A., Dua, R., Haider, W., et al. (2015). Surface Modification of Ni-Ti Alloys for Stent Application after Magnetoelectropolishing. *Mater. Sci. Eng. C* 50, 37–44. doi:10.1016/j.msec.2015.01.009

Hahn, A., Fuhlrott, J., Loos, A., and Barcikowski, S. (2012). Cytotoxicity and Ion Release of alloy Nanoparticles. *J. Nanopart Res.* 14 (1). doi:10.1007/s11051-011-0686-3

Hamann, I., Hempel, U., Rotsch, C., and Leimert, M. (2020). Biological Cell Investigation of Structured Nitinol Surfaces for the Functionalization of Implants. *Materials* 13 (15), 3264–3275. doi:10.3390/MA13153264

Hoshyar, N., Gray, S., Han, H., and Bao, G. (2016). The Effect of Nanoparticle Size on *In Vivo* Pharmacokinetics and Cellular Interaction. *Nanomedicine* 11 (6), 673–692. doi:10.2217/nnm.16.5

Hou, X., Mankoci, S., Walters, N., Gao, H., Zhang, R., Li, S., et al. (2018). Hierarchical Structures on Nickel-Titanium Fabricated by Ultrasonic Nanocrystal Surface Modification. *Mater. Sci. Eng. C* 93, 12–20. doi:10.1016/j.msec.2018.07.032

Ion, R., Luculescu, C., Cimpean, A., Marx, P., Gordin, D.-M., and Gloriant, T. (2016). Nitride Coating Enhances Endothelialization on Biomedical NiTi Shape Memory alloy. *Mater. Sci. Eng. C* 62, 686–691. doi:10.1016/j.msec.2016.02.031

Jeevanandam, J., Barhoum, A., Chan, Y. S., Dufresne, A., and Danquah, M. K. (2018). Review on Nanoparticles and Nanostructured Materials: History, Sources, Toxicity and Regulations. *Beilstein J. Nanotechnol.* 9, 1050–1074. doi:10.3762/bjnano.9.98

Kashapov, R., Ibragimova, A., Pavlov, R., Gabdrakhmanov, D., Kashapova, N., Burilova, E., et al. (2021). Nanocarriers for Biomedicine: From Lipid Formulations to Inorganic and Hybrid Nanoparticles. *Ijms* 22 (13), 7055. doi:10.3390/ijms22137055

Kum, K.-Y., and Chang, S. W. (2017). The Effect of Hydrofluoric Acid Surface Treatment on the Cyclic Fatigue Resistance of K3 NiTi Instruments. *Bioinorganic Chem. Appl.* 2017, 1–6. doi:10.1155/2017/3189729

Kyriakides, T. R., Raj, A., Tseng, T. H., Xiao, H., Nguyen, R., Mohammed, F. S., et al. (2021). Biocompatibility of Nanomaterials and Their Immunological Properties. *Biomed. Mater.* 16 (4), 042005. doi:10.1088/1748-605X/abe5fa

Loza, K., Heggen, M., and Epple, M. (2020). Synthesis, Structure, Properties, and Applications of Bimetallic Nanoparticles of Noble Metals. *Adv. Funct. Mater.* 30 (21), 1909260. doi:10.1002/adfm.201909260

McNamara, K., and Tofail, S. A. M. (2017). Nanoparticles in Biomedical Applications. *Adv. Phys. X* 2, 54–88. doi:10.1080/23746149.2016.1254570

Mirjalili, M., Momeni, M., Ebrahimi, N., and Moayed, M. H. (2013). Comparative Study on Corrosion Behaviour of Nitinol and Stainless Steel Orthodontic Wires in Simulated Saliva Solution in Presence of Fluoride Ions. *Mater. Sci. Eng. C* 33 (4), 2084–2093. doi:10.1016/j.msec.2013.01.026

Mohammadi, F., Golafshan, N., Kharaziha, M., and Ashrafi, A. (2019). Chitosan-heparin Nanoparticle Coating on Anodized NiTi for Improvement of Blood Compatibility and Biocompatibility. *Int. J. Biol. Macromolecules* 127, 159–168. doi:10.1016/j.ijbiomac.2019.01.026

Nagaraja, S., and Pelton, A. R. (2020). Corrosion Resistance of a Nitinol Ocular Microstent: Implications on Biocompatibility. *J. Biomed. Mater. Res.* 108 (6), 2681–2690. doi:10.1002/jbm.b.34599

Norouzi, N., and Nouri, Z. (2021). The Effect of Two-Stage Acid Treatment on Surface Behavior and Improvement of Bioactivity of Nitinol alloy. *Biointerface Res. Appl. Chem.* 11 (3), 10690–10702. doi:10.33263/BRIAC113.1069010702

Oncel, L., and Acma, M. E. (2017). Effect of Heat Treatment Temperature and Heat Treatment Time on Properties and Use of NiTi Shape Memory Implant Material. *Int. Adv. Res. J. Sci. Eng. Tech.* 4 (1), 64–69. doi:10.17148/iarjset.2017.4115

Osfouri, M., and Rahmani, O. (2021). Nitinol Wire-Reinforced GLAREs as a Novel Impact Resistant Material: An Experimental Study. *Compos. Structures* 276, 114521. doi:10.1016/j.compstruct.2021.114521

Parmar, V., Singh, S., Kumar, S., Vijaya Prakash, G., and Kalyanasundaram, D. (2021). Thermo-physical Modeling and Experimental Validation of Core-Shell Nanoparticle Fabrication of Nickel-Titanium (Nitinol) alloy. *Opt. Laser Tech.* 138, 106880. doi:10.1016/j.optlastec.2020.106880

Pérez, L. M., Gracia-Villa, L., Puértolas, J. A., Arruebo, M., Irusta, S., and Santamaría, J. (2009). Effect of Nitinol Surface Treatments on its Physico-Chemical Properties. *J. Biomed. Mater. Res.* 91B (1), 337–347. doi:10.1002/jbm.b.31407

Phan, H. T., and Haes, A. J. (2019). What Does Nanoparticle Stability Mean? *J. Phys. Chem. C* 123 (27), 16495–16507. doi:10.1021/acs.jpcc.9b00913

Pugazhendhi, A., Edison, T. N. J. I., Karuppusamy, I., and Kathirvel, B. (2018). Inorganic Nanoparticles: A Potential Cancer Therapy for Human Welfare. *Int. J. Pharmaceutics* 539 (1-2), 104–111. doi:10.1016/j.ijpharm.2018.01.034

Pulletikurthi, C., Munroe, N., Stewart, D., Haider, W., Amruthaluri, S., Rokicki, R., et al. (2015). Utility of Magneto-Electropolished Ternary Nitinol Alloys for Blood Contacting Applications. *J. Biomed. Mater. Res.* 103 (7), 1366–1374. doi:10.1002/jbm.b.33317

Rahimipour, S., Salahinejad, E., Sharifi, E., Nosrati, H., and Tayebi, L. (2020). Structure, Wettability, Corrosion and Biocompatibility of Nitinol Treated by Alkaline Hydrothermal and Hydrophobic Functionalization for Cardiovascular Applications. *Appl. Surf. Sci.* 506, 144657. doi:10.1016/j.apsusc.2019.144657

Safranski, D., Dupont, K., and Gall, K. (2020). Pseudoelastic NiTiNOL in Orthopaedic Applications. *Shap. Mem. Superelasticitysuperelasticity* 6, 332–341. doi:10.1007/s40830-020-00294-y

Sena, G. M., Sivan, S., Weaver, J. D., and Di Prima, M. (2020). Larger Surface Area Can Reduce Nitinol Corrosion Resistance. *Npj Mater. Degrad.* 4, 23. doi:10.1038/s41529-020-00128-3

Sevost'yanov, M. A., Nasakina, E. O., Baikin, A. S., Sergienko, K. V., Konushkin, S. V., Kaplan, M. A., et al. (2018). Biocompatibility of New Materials Based on Nano-Structured Nitinol with Titanium and Tantalum Composite Surface Layers: Experimental Analysis *In Vitro* and

In Vivo. *J. Mater. Sci. Mater. Med.* 29 (3), 33. doi:10.1007/s10856-018-6039-3

Shabalovskaya, S. A., Anderegg, J. W., Undisz, A., Rettenmayr, M., and Rondelli, G. C. (2012). Corrosion Resistance, Chemistry, and Mechanical Aspects of Nitinol Surfaces Formed in Hydrogen Peroxide Solutions. *J. Biomed. Mater. Res.* 100B (6), 1490–1499. doi:10.1002/jbm.b.32717

Shannahan, J. (2017). The Biocorona: A challenge for the Biomedical Application of Nanoparticles. *Nanotechnol. Rev.* 6 (4), 345–353. doi:10.1515/ntrev-2016-0098

Ulacia, P., Rimac, G., Lalancette, S., Belleville, C., Mongrain, R., Plante, S., et al. (2020). A Novel Fiber-optic Based 0.014″ Pressure Wire: Designs of the OptoWire , Development Phases, and the O 2 First-in-man Results. *Cathet Cardio Intervent* 99 (59)), 67–69. doi:10.1002/ccd.29321

Zelepukin, I. V., Popov, A. A., Shipunova, V. O., Tikhonowski, G. V., Mirkasymov, A. B., Popova-Kuznetsova, E. A., et al. (2021). Laser-synthesized TiN Nanoparticles for Biomedical Applications: Evaluation of Safety, Biodistribution and Pharmacokinetics. *Mater. Sci. Eng. C* 120, 111717. doi:10.1016/j.msec.2020.111717

Conflict of Interest: The authors declare that the research was conducted in the absence of any commercial or financial relationships that could be construed as a potential conflict of interest.

Publisher's Note: All claims expressed in this article are solely those of the authors and do not necessarily represent those of their affiliated organizations, or those of the publisher, the editors, and the reviewers. Any product that may be evaluated in this article, or claim that may be made by its manufacturer, is not guaranteed or endorsed by the publisher.